ELSEVIER

Solid State Ionics 108 (1998) 363–370

SOLID STATE IONICS

Development of mixed-conducting oxides for gas separation

U. Balachandran[a,*], B. Ma[a], P.S. Maiya[a], R.L. Mieville[a], J.T. Dusek[a], J.J. Picciolo[a], J. Guan[a], S.E. Dorris[a], M. Liu[b]

[a]*Energy Technology Division, Argonne National Laboratory, Argonne, Illinois 60439, USA*
[b]*School of Materials Science and Engineering, Georgia Institute of Technology, Atlanta, Georgia 30332, USA*

Abstract

Mixed-conducting oxides have been used in many applications, including fuel cells, gas-separation membranes, sensors, and electrocatalysis. We are developing a mixed-conducting, dense ceramic membrane for selectively transporting oxygen and hydrogen. Ceramic membranes made of Sr-Fe-Co oxide, which has high combined electronic and oxygen ionic conductions, can be used to selectively transport oxygen during the partial oxidation of methane to synthesis gas (syngas, $CO + H_2$). We have measured the steady-state oxygen permeability of $SrFeCo_{0.5}O_x$ as a function of oxygen partial-pressure gradient and temperature. At 900°C, oxygen permeability was ≈ 2.5 scc $\cdot$ cm^{-2} $\cdot$ min^{-1} for a 2.9 mm thick membrane and this value increases as membrane thickness decreases. We have fabricated tubular $SrFeCo_{0.5}O_x$ membranes and operated them at 900°C for >1000 h during conversion of methane into syngas. The hydrogen ion (proton) transport properties of $Ba(Ce,Y)O_{3-\delta}$ were investigated by impedance spectroscopy and open-cell voltage measurements. High proton conductivity and a high protonic transference number make $Ba(Ce,Y)O_{3-\delta}$ a potential membrane for hydrogen separation. Published by Elsevier Science B.V.

Keywords: Mixed-conductor; Gas separation; Oxygen permeation; Proton conduction; Ceramic membrane

1. Introduction

In recent years, mixed-conducting oxides, in which both ionic and electronic charge carriers exist, have received increased attention because of their technological importance in high-temperature electrochemical devices and in electrocatalysis. For example, they are used as sensors and as electrodes in solid-state fuel cells; if their ionic conductivity is high enough, they can be used as dense membranes for gas separation. It is generally accepted that mixed-conducting oxide membranes have great potential to meet the needs of many segments of the oxygen market. The applications envisioned range from small-scale oxygen pumps for medical applications to large-scale usage in combustion processes such as coal liquefaction. In the early 1980s, Iwahara et al. [1–3] first reported protonic conduction in $SrCeO_3$ materials. Later, the $BaCeO_3$ system was extensively studied because of its higher conductivities [4–7]. Following their discovery by Teraoka et al. [8,9] in the late 1980s, mixed-conducting perovskites with combined electronic and oxide ionic conductivities and appreciable oxygen permeability have been investigated [10–15]. Recently, Balachandran et al. [16,17] have shown that Sr-Fe-Co oxides exhibit not only high combined electronic and oxy-

*Corresponding author. Tel: +1 630 252-4250: fax: +1 630 252-3604: e-mail: u_balachandran@qmgate.anl.gov

0167-2738/98/$19.00 Published by Elsevier Science B.V.
PII S0167-2738(98)00064-2

gen ionic conductivities but also structural stability. Extruded tubes of these materials have been evaluated in a reactor operating at $\approx 850°C$ to convert methane to syngas in the presence of a reforming catalyst. Methane conversion coefficients $>98\%$ [18,19] were observed, and some of the reactor tubes have been operated for more than 1000 h.

In this paper, we report our recent results on Sr-Fe-Co-O oxygen permeable and $Ba(Ce,Y)O_{3-\delta}$ proton-conducting membrane materials. Oxygen permeation flux was measured as a function of oxygen partial pressure (p_{O_2}) difference and temperature. Oxygen permeation data obtained from an actual methane conversion reactor is compared with the steady-state oxygen permeation data measured with a gas-tight electrochemical cell. Hydrogen transport has been studied by impedance spectroscopy and open-cell voltage (OCV) methods.

2. Experimental

Oxygen-ion conductor $SrFeCo_{0.5}O_x$ (SFC) samples were prepared by a solid-state reaction method with $SrCO_3$, Fe_2O_3, and $Co(NO_3)_2 \cdot 6H_2O$ as starting materials. Mixing and grinding were performed in isopropanol with zirconia medium. After drying, the mixtures were calcined at $\approx 850°C$ for 16 h in air with intermittent grinding. Phase purity was confirmed by X-ray diffraction (XRD). The resulting powders were pressed into pellets and sintered in air at 1200°C for 5 h. Sintered pellets were polished and used for permeation tests. Proton conductor $BaCe_{0.95}Y_{0.5}O_3$ (BCY) was also prepared by a solid-state reaction method. Initial chemicals ($BaCO_3$, CeO_2 and Y_2O_3) were mixed in the desired mole ratios and ball-milled in isopropanol for at least 24 h and then calcined at 1000°C for 12 h in air. The obtained powders were ground and recalcined at 1200°C for 10 h in air. The resulting powders were examined by XRD, and pressed uniaxially with a 100 MPa load into pellets 22.5 mm in diameter and ≈ 2 mm thick. The pellets were then sintered in air at 1550°C for 10 h.

Total and oxygen ionic conductivities of SFC were measured as a function of p_{O_2} by conventional and electron-blocking four-probe methods [17,20], respectively. The experimental setup used to study oxygen permeation of SFC membranes has been reported earlier [21]. A sintered pellet of SFC was sealed to a yttria-stabilized zirconia (YSZ) crucible by a Pyrex glass seal. Oxygen-permeable electrodes were placed on the bottom and side of the YSZ crucible (as shown in Fig. 1). The bottom electrodes were used to pump oxygen from the gas-tight cell, while the other electrodes were used to detect the p_{O_2} inside the cell. The p_{O_2} inside the cell can be determined from the electromotive force (EMF), E, generated on the side wall of the YSZ crucible by solving the following equation:

$$p_{O_2^{II}} = p_{O_2^{I}} \exp\left(\frac{4FE}{RT}\right) \tag{1}$$

where $p_{O_2^{II}}$ and $p_{O_2^{I}}$ are the p_{O_2} values inside and outside the gas-tight cell, respectively. Other variables are as usual, i.e., F, Faraday's constant; R, gas constant; and T, absolute temperature.

The experimental setup for investigating proton transport in the BCY samples is illustrated in Fig. 2. Platinum mesh (#80) was cut to the appropriate size and attached to both polished sides of a sintered specimen. The specimen and platinum mesh were then heated to 150°C and kept at that temperature for 2 h, then heated at 850°C for 30 min for conditioning. Subsequently, the specimen was sealed with a glass sealant onto one end of the inner alumina tube of the setup [22]. The glass powder

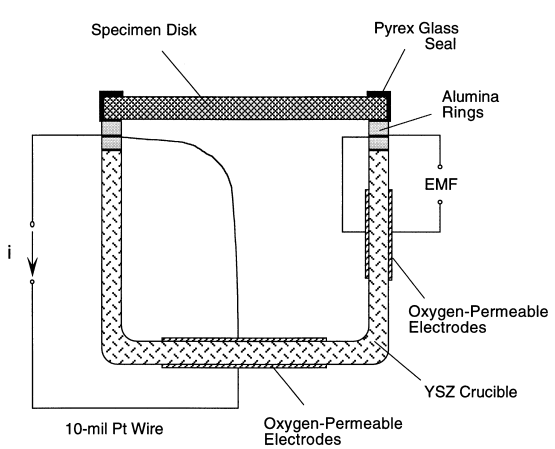

Fig. 1. Schematic drawing of cross-sectional view of gas-tight electrochemical cell used to measure oxygen permeability.

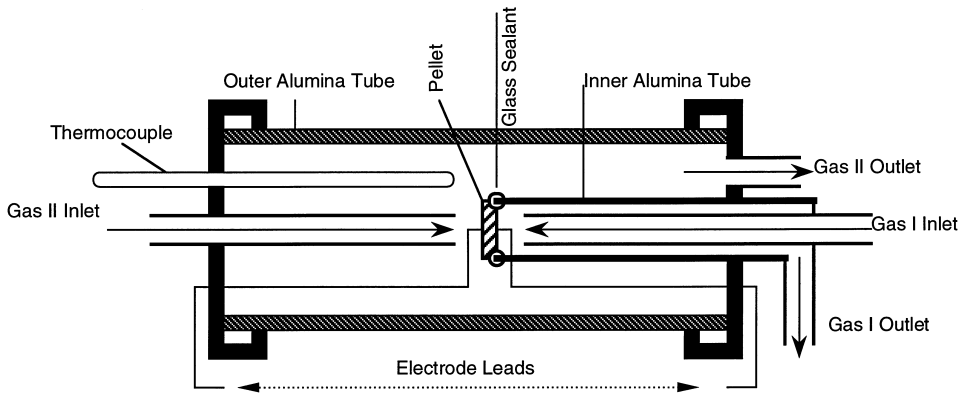

Fig. 2. Schematic illustration of experimental setup for testing proton conductors.

was mixed with ethylene glycol as binder and isopropyl alcohol as dispersant. The sealed structure was first air-dried, then heated slowly (20°C/h ramp and 5 h dwell at 350°C) to burn out the binder, and finally devitrified at 780°C. The two-point method was used to measure the impedance spectra of the specimens and, thus, to determine the total conductivity. Ionic transference numbers were derived from OCV after exposing two sides of the specimen to different gaseous environments [23]. Gas flowrates were controlled to $\approx$100 scc·min^{-1}.

3. Results and discussion

3.1. Oxygen ionic conductor SFC

By using the conventional four-probe and electron-blocking four-probe methods, we measured the total and ionic conductivities of SFC. Electronic conductivity can be deduced by subtracting ionic conductivity from the total conductivity. The results obtained in air at high temperatures showed that the electronic and ionic conductivities of the SFC sample are comparable, or, in another words, their ratio is close to unity. This makes SFC materials unique among other mixed conductors, in which electronic transference numbers are much greater than ionic transference numbers, or vice versa. The oxygen permeation flux j_{O_2}, through a membrane of thickness L can be deduced from conductivity data [20] as follows:

$$j_{O_2} = \frac{RT}{16F^2L} \int_{p^{I}_{O_2}}^{p^{II}_{O_2}} \sigma_{tot} t_{ion} t_{el} \, d \ln(p_{O_2}) \quad (2)$$

where σ_{tot} is total conductivity, t_{ion} is ionic transference number, and t_{el} is electronic transference number. The oxygen permeability of SFC was determined by using a gas-tight cell described earlier [20]. Reducing oxygen environments were achieved by pumping oxygen out from the gas-tight cell by pumping electrodes on the YSZ crucible. Oxygen permeates the SFC disk membrane because of the p_{O_2} difference. Under steady-state conditions, the amount of oxygen that enters the cell (by permeating through the specimen disk) is equal to that pumped out by the YSZ oxygen pump. Therefore, the flow of oxygen through the specimen can be determined by the current applied to the YSZ oxygen pump. Oxygen permeation flux j_{O_2} is related to the applied current I by:

$$j_{O_2} = \frac{I}{4FS} \quad (3)$$

where S is the effective cross-sectional area of the specimen. Oxygen permeation flux through a 2.9 mm thick SFC disk at 900°C obtained by using Eq. (3), the experimental data of a steady-state pumping current I, and geometric parameters of the specimen, is plotted in Fig. 3 as a function of the p_{O_2} inside the gas-tight cell. Flowing air (p_{O_2}=0.21 atm) was the

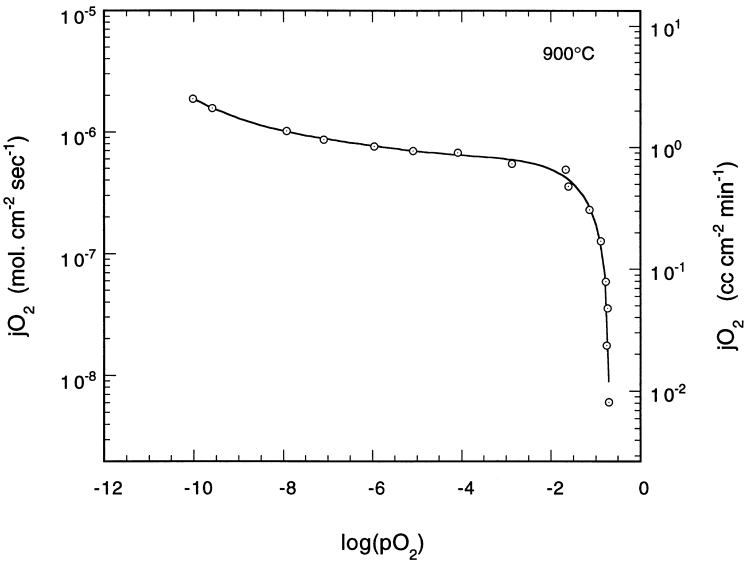

Fig. 3. Oxygen permeation flux as a function of oxygen partial pressure inside a gas-tight cell, with air as outside reference atmosphere. Specimen thickness = 2.9 mm.

reference atmosphere (outside the gas-tight cell) during oxygen permeation experiments. Fig. 3 shows that j_{O_2} increases dramatically in the range between $p_{O_2} = 0.21$ and $\approx 10^{-3}$ atm, and its slope becomes flatter when p_{O_2} inside the cell is reduced further. Results on oxygen permeability at various p_{O_2} gradients and temperatures show that j_{O_2} increases, as expected, with temperature and p_{O_2} gradients. At 900°C, oxygen permeability was found to be ≈ 2.5 $scc \cdot cm^{-2} \cdot min^{-1}$ for a 2.9 mm thick specimen and increases as membrane thickness decreases.

Sintered thin-wall tubes of SFC were tested in a methane conversion reactor for >1000 h [18,19,24]. Oxygen permeation flux determined from reactor experiments (with tubular SFC membrane) [24] and determined from experiments with a gas-tight electrochemical cell have been plotted in Fig. 4 as a function of temperature. The wall thickness of tubular membrane used in methane conversion reactor was 0.75 mm. The permeation flux determined from gas-tight electrochemical cell was normalized to that of a 0.75 mm thick membrane for comparison with the data obtained from methane conversion reactor. Results from these two independent experiments are in good agreement with each other.

3.2. Protonic conductor BCY

Fig. 5 shows the total conductivity of BCY in various atmospheres, as determined by impedance spectroscopy. The total conductivity of $BaCeO_{0.95}Y_{0.05}O_{3-\delta}$ was low in pure argon, even at high temperatures (≥600°C), but increased slightly with addition of 2% water vapor in the surrounding environment. The total conductivity of BCY was found to be higher in pure oxygen than in pure argon. At low temperatures, addition of water increases the total conductivity, whereas at high temperatures, total conductivity slightly decreased when water vapor was added. Total conductivity of the BCY sample increases from $\approx 5 \times 10^{-3}$ $\Omega^{-1} \cdot cm^{-1}$ to $\approx 2 \times 10^{-2}$ $\Omega^{-1} \cdot cm^{-1}$ at 600°C.

Transference numbers in an oxygen-containing atmosphere were determined by using the following concentration cells:

$$\text{II, } O_2 + 2.81\%H_2O, \text{ Pt}|\text{BCY}|\text{Pt, } N_2 + 8\%O_2 + 2.81\%H_2O, \text{ I,} \quad \text{(c1)}$$

$$\text{II, } O_2 + 7.38\%H_2O, \text{ Pt}|\text{BCY}|\text{Pt, } N_2 + 8\%O_2 + 2.64\%H_2O, \text{ I,} \quad \text{(c2)}$$

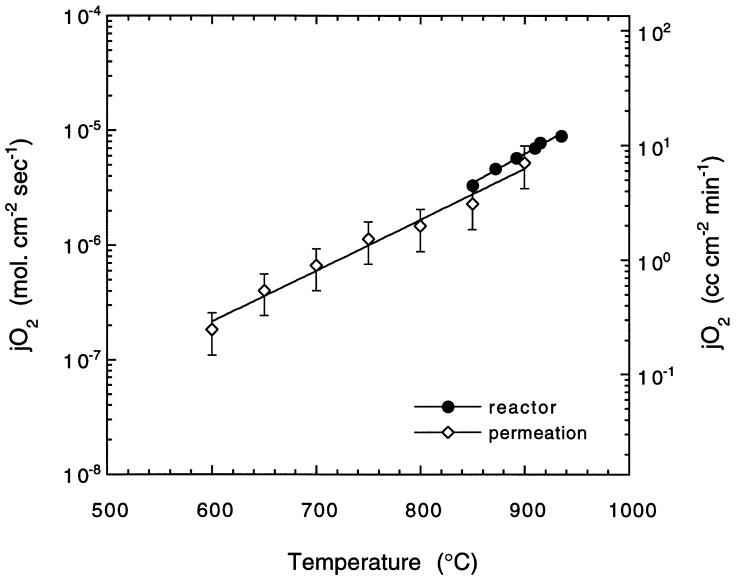

Fig. 4. Temperature dependence of oxygen permeation flux determined by two independent methods, gas-tight electrochemical cell and methane conversion reactor.

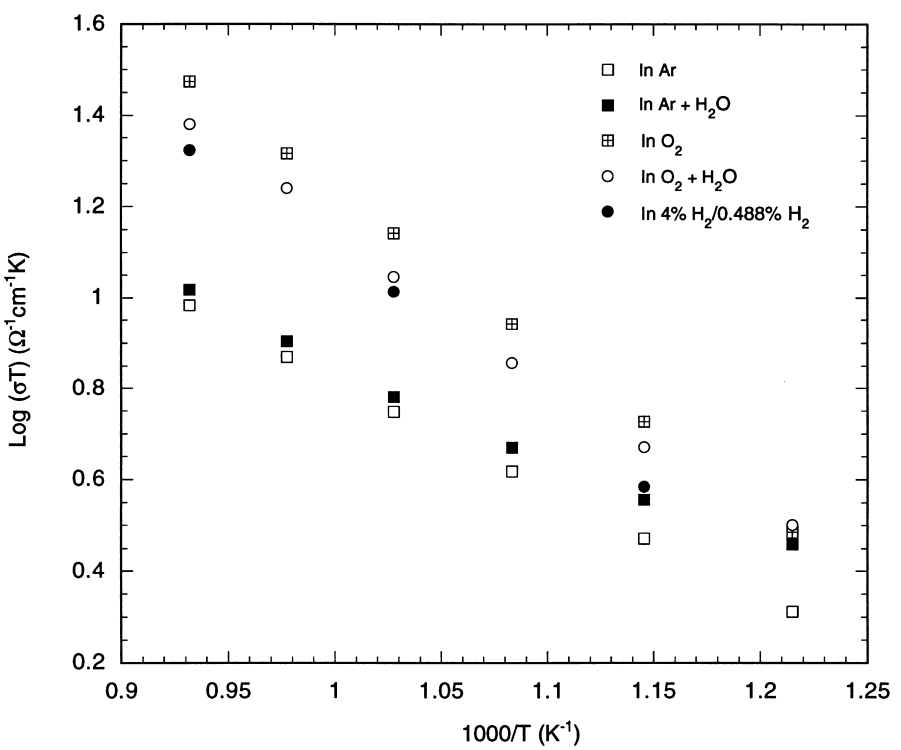

Fig. 5. Total conductivity of $BaCe_{0.95}Y_{0.05}O_{3-\delta}$ sample measured in various atmospheres.

Table 1
Open-cell voltages (mV) of oxygen/water vapor concentration cells at various temperatures

Temperature (°C)	Cell 1	Cell 2	Cell 3
500	32.0	14.8	−48.2
600	28.0	19.9	−36.8
700	27.2	22.1	−31.3
800	26.4	22.3	−29.7

II, $N_2 + 8\%O_2 + 7.38\%H_2O$, Pt|BCY|Pt, $N_2 + 2.81\%H_2O$, I. (c3)

As shown in Table 1, the measured OCVs of Cell 1 decreased as temperature increased, indicating that the electronic transference number increases with temperature. In Cell 2, where the OCV was solely due to the partial-pressure difference of water vapor, the OCVs are directly related to the protonic transference number according to following equation [23]:

$$V_{OC} = \frac{RT}{4F}\left[t_{ion} \ln\left(\frac{p^{II}_{O_2}}{p^{I}_{O_2}}\right) - 2t_{H^+} \ln\left(\frac{p^{II}_{H_2O}}{p^{I}_{H_2O}}\right)\right] \quad (4)$$

where $t_{ion} = t_{H^+} + t_{O_2^-}$ is the ionic transference number. The transference numbers obtained in Eq. (4) are plotted in Fig. 6, which shows that the protonic transference number decreases whereas the electronic transference number increases with increasing temperature.

Transference numbers in hydrogen/water vapor atmospheres were studied by employing the following cells:

II, $N_2 + 4\%H_2 + 2.64\%H_2O$, Pt|BCY|Pt, $N_2 + 0.488\%H_2 + 2.64\%H_2O$, I, (c4)

II, $N_2 + 4\%H_2 + 7.38\%H_2O$, Pt|BCY|Pt, $N_2 + 0.488\%H_2 + 2.64\%H_2O$, I, (c5)

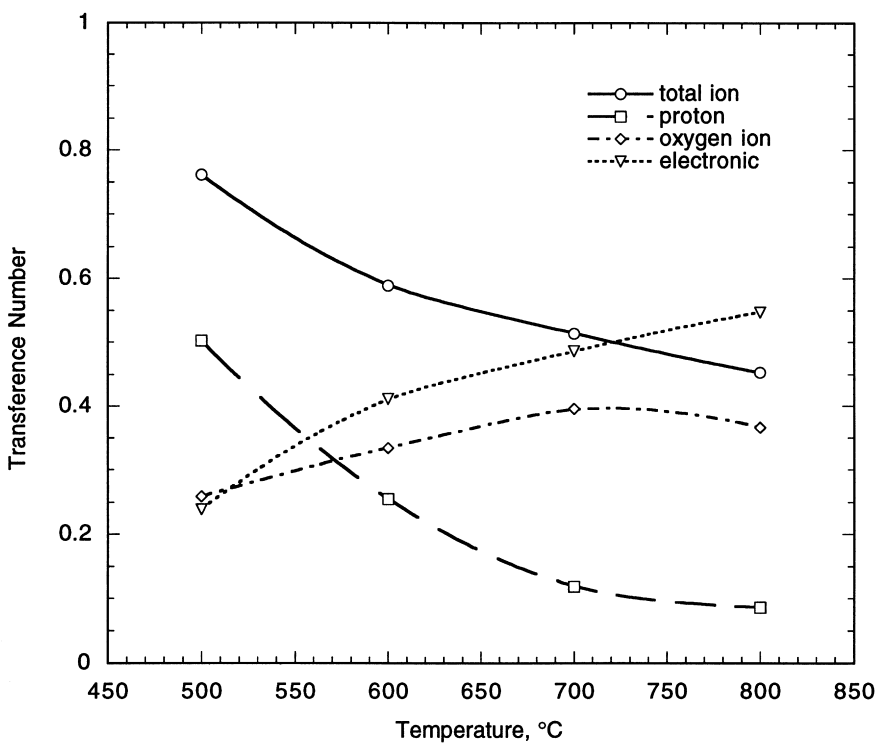

Fig. 6. Transference numbers of $BaCe_{0.95}Y_{0.05}O_{3-\delta}$ sample as determined in oxygen-containing environments.

Table 2
Open-cell voltages (mV) of hydrogen/water vapor concentration cells at various temperatures

Temperature (°C)	Cell 4	Cell 5	Cell 6
500	−63.13	−62.01	64.02
600	−66.43	−64.48	68.14
700	−70.55	−65.17	75.57
800	−76.39	−69.11	83.26

II, N_2 + 0.488%H_2 + 7.38%H_2O, Pt|BCY|Pt, N_2 + 4%H_2 + 2.64%H_2O, I. (c6)

The obtained OCVs are listed in Table 2, and the ionic transference numbers were derived by solving following equation [23]:

$$V_{OC} = \frac{RT}{4F}\left[- t_{ion} \ln\left(\frac{p^{II}_{H_2}}{p^{I}_{H_2}}\right) + t_{O^{2-}} \ln\left(\frac{p^{II}_{H_2O}}{p^{I}_{H_2O}}\right)\right]. \quad (5)$$

The obtained transference numbers are plotted in Fig. 7. Again, the protonic transference number decreases whereas the electronic transference number increases with increasing temperature. The protonic transference number decreases from 0.87 to 0.63, whereas the oxygen transference number increases from 0.03 to 0.15 as temperature increases from 600 to 800°C in the hydrogen/water vapor atmospheres.

4. Conclusions

A mixed-conducting ceramic, $SrFeCo_{0.5}O_x$ (SFC), has been developed. It exhibits high electronic and oxygen ionic conductivities, and its electronic and ionic transference number are comparable, making it unique among other mixed conductors. The oxygen permeability of membranes made of the SFC material is high. Direct measurement of oxygen permeation flux with a gas-tight electrochemical cell is in good agreement with the values obtained from methane

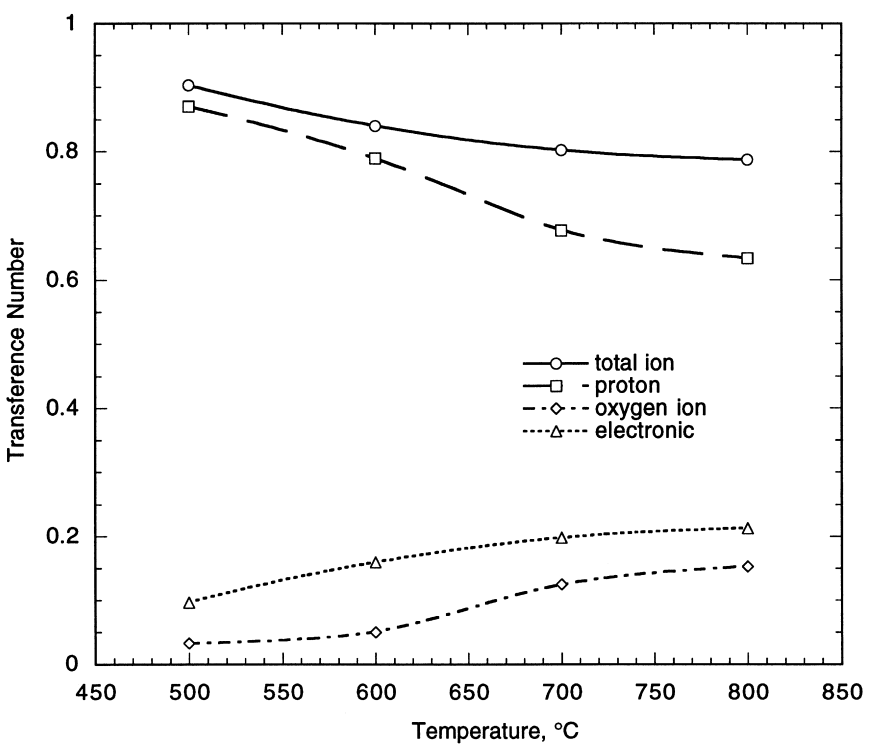

Fig. 7. Transference numbers of $BaCe_{0.95}Y_{0.05}O_{3-\delta}$ sample as determined in hydrogen-containing environments.

conversion reaction experiments. Oxygen permeation flux, as determine with a gas-tight electrochemical cell, was $\approx$2.5 scc$\cdot$cm$^{-2}\cdot$min^{-1} for a 2.9 mm thick specimen at 900°C. Oxygen permeability of the SFC membranes increases with increasing temperature and decreasing membrane thickness.

Transport properties of $BaCe_{0.95}Y_{0.05}O_{3-\delta}$ were studied with impedance spectroscopy and open-cell voltage (OCV) measurements. Proton conduction has been observed in this material in hydrogen-containing atmospheres. Proton and oxygen transference numbers, deduced from OCV data, showed that the protonic transference numbers decrease whereas the electronic transference number increase with increasing temperature. Total conductivity of the BCY sample increased from $\approx 5\times10^{-3}$ $\Omega^{-1}\cdot$cm^{-1} to $\approx 2\times10^{-2}$ $\Omega^{-1}\cdot$cm^{-1} at 600°C, whereas the protonic transference number decreased from 0.87 to 0.63 and the oxygen transference number increased from 0.03 to 0.15 as temperature increased from 600 to 800°C in hydrogen/water vapor atmospheres.

Acknowledgements

This work was supported by the U.S. Department of Energy, Federal Energy Technology Center, under Contract W-31-109-Eng-38.

References

[1] H. Iwahara, T. Esaka, H. Uchida, N. Maeda, Solid State Ionics 3–4 (1981) 359.
[2] T. Yajima, H. Suzuki, T. Yogo, H. Iwahara, Solid State lonics 51 (1992) 101.
[3] H. Iwahara, Solid State Ionics 77 (1995) 289.
[4] J.F. Liu, A.S. Nowick, Mater. Res. Soc. Symp. Proc. 210 (1991) 673.
[5] N. Bonanos, Solid State Ionics 53–56 (1992) 967.
[6] N. Taniguchi, K. Hatoh, J. Niikura, T. Gamo, Solid State Ionics 53,56 (1992) 998.
[7] D.A. Steveson, N. Jiang, R.M. Buchanan, F.E.G. Henn, Solid State Ionics 62 (1993) 279.
[8] Y. Teraoka, H. Zhang, S. Furukawa, N. Yamazoe, Chem. Lett. (1985) 1743.
[9] Y. Teraoka, H. Zhang, K. Okamoto, N. Yamazoe, Mater. Res. Bull. 23 (1988) 51.
[10] Y. Nigara, J. Mizusaki, M. Ishigame, Solid State Ionics, 9 (1995) 208.
[11] H. Arashi, H. Naito, M. Nakata, Solid State Ionics 76 (1995) 315.
[12] R.H.E. Van Doorn, H. Kruidhof, H.J.M. Bouwmeester, A.J. Burggraaf, Mater. Res. Soc. Symp. Proc. 369 (1991) 377.
[13] Y. Teraoka, T. Nobunaga, K. Okamoto, N. Miura, N. Yamazoe, Solid State Ionics 48 (1991) 207.
[14] H.W. Brinkman, H. Kruidhof, A.J. Burggraaf, Solid State Ionics 68 (1994) 173.
[15] U. Balachandran, S.L. Morissette, J.T. Dusek, R.L. Mieville, R.B. Poeppel, M.S. Kleefisch, S. Pei, T.P. Kobylinski, C.A. Udovich in: S. Rogers et al. (Eds.), Proc. Coal Liquefaction and Gas Conversion Contractor Review Conf. U.S Dept. of Energy, Pittsburgh Energy Technology Center 1, 1993, pp. 138–160.
[16] U. Balachandran, M.S. Kleefsch, T.P. Kobylinski, S.L. Morissette, S. Pei, U.S. Patent 5580497, Dec. 1996.
[17] B. Ma, J.-H. Park, C.U. Segre, U. Balachandran, Mater Res. Soc. Symp. Proc. 393 (1995) 49.
[18] U. Balachandran, T.J. Dusek, S.M. Sweeney, R.B. Poeppel, R.L. Mieville, P.S. Maiya, M.S. Kleefisch, S. Pei, T.P. Kobylinski, C.A. Udovich, A.C. Bose, Am. Ceram. Soc. Bull. 74 (1995) 71.
[19] U. Balachandran, J.T. Dusek, P.S. Maiya, B. Ma, R.L. Mieville, M.S. Kleefisch, C.A. Udovich, Catalysis Today 36 (1997) 265.
[20] B. Ma, U. Balachandran, J.-H. Park, J. Electrochem. Soc. 143 (1996) 1736.
[21] B. Ma, U. Balachandran, C.-C. Chao, J.-H. Park, Ceram. Trans. 73 (1997) 169.
[22] K.L. Ley, M. Krumplet, R. Kumar, J.H. Meiser, I. Bloom, J. Mater Res. 11 (1996) 1489.
[23] J. Guan, S.E. Dorris, U. Balachandran, M. Liu, Solid State Ionics 100 (1997) 45.
[24] P.S. Maiya, U. Balachandran, J.T. Dusek, R.L. Mieville, M.S. Kleefisch, C.A. Udovich, Solid State Ionics 99 (1997) 1.